Computations and Parameterizations of the Nonlinear Energy Transfer in a Gravity-Wave Spectrum. Part I: A New Method for Efficient Computations of the Exact Nonlinear Transfer Integral

S. HASSELMANN AND K. HASSELMANN

Max-Planck-Institut für Meteorologie, Hamburg, Federal Republic of Germany

(Manuscript received 17 September 1984, in final form 30 April 1985)

ABSTRACT

A more efficient method of computing the nonlinear transfer in a surface wave spectrum is developed which is symmetrical with respect to all wavenumbers of the resonant interaction quadruplets. This enables a large number of computations to be carried out, as required for investigations of the spectral energy balance or the development of parameterizations. New results are presented for finite-depth surface waves. By filtering out regions in interaction phase space, the assumptions involved in the narrow-peak and local-interaction approximations are investigated. Both approximations are found to be useful but are generally not sufficiently accurate to replace exact computations or provide adequate parameterizations for wave models.

1. Introduction

The nonlinear transfer of energy by resonant wave–wave interactions is known to play an important role in the spectral energy balance of wind waves. However, it has not yet been possible to represent this process satisfactorily in numerical wave models. Although the basic mechanism of the transfer has long been well understood (Hasselmann, 1962, 1963a) and numerical calculations of the transfer rate for particular spectra have been presented in a number of papers (Hasselmann, 1963b; Cartwright, 1968; Sell and Hasselmann, 1972; Webb, 1978; Masuda, 1981) exact computations of the full five-dimensional Boltzmann transfer-integral expression are far too time consuming for incorporation in wave models. In fact, the excessive computing requirements have in the past even precluded systematic transfer calculations for a sufficiently wide variety of spectra to develop and test suitable parameterizations of the exact expression for use in wave models.

In Part I of this two-part paper we describe a method of computing the nonlinear transfer based on a symmetrical treatment of the interactions which is one to two orders of magnitude more efficient than previous methods. With the new technique, large series of exact computations can now be carried out, enabling the systematic development of parameterizations of the nonlinear transfer, described in Part II of this paper (Hasselmann *et al.*, 1985).

The need for improved parameterizations of the nonlinear transfer in wave models (cf. The SWAMP Group, 1985) is not the only motivation for developing a more efficient method of computing the exact transfer expression. Although the general structure of the energy balance of a growing wind sea is believed now to be fairly well understood, a number of details have still not been determined quantitatively. This applies particularly to the form of the dissipation source function. The problem can be approached by numerical energy balance experiments, in which the knowledge that is available on the form of the input source function, the nonlinear transfer and the observed growth of fetch-limited spectra is used to infer the form of the residual dissipation source function. In order to compare the observed and theoretical growth curves, the spectral transport equation must be integrated with respect to fetch for a given set of assumed source functions. This is feasible only if an efficient method of evaluating the exact nonlinear transfer expression is available. (The alternative strategy of differentiating the observed growth curves and comparing these with the theoretical source functions computed at a few fixed fetch locations is found to be too sensitive with respect to small variations in the spectral shape.) Komen *et al.* (1984) have carried out such numerical experiments to investigate the structure of the energy balance of a fully developed spectrum, using the computational techniques described here, and determined the form of dissipation source functions needed to maintain the observed fully developed spectrum. Similar results for fetch-limited wave growth are summarized by Hasselmann and Hasselmann (1985). Young *et al.* (1985a) have carried out energy balance experiments with essentially the same model to investigate the directional response of the wave spectrum to turning winds. Numerical integrations of this kind, based on the exact nonlinear transfer source function, at the same time provide an important contribution to the reference data set for

testing and calibrating the parameterization schemes discussed in Part II.

The basic method of computation is described in Section 2. For a more detailed description of numerical details and an extensive compilation of computed transfer rates for a variety of spectral shapes we refer to the report by Hasselmann and Hasselmann (1981). Results for the special case of cross-sea interactions are given by Young *et al.* (1985b).

In Section 3 we summarize briefly the principal features of these computations that are important for understanding the role of the nonlinear transfer in controling the spectral shape and rate of development of a growing wind-wave spectrum, and the adjustment of the wave spectrum to changing winds. These features must be reproduced by a satisfactory parameterization scheme. In Section 4 we present as examples the nonlinear transfer computed for finite-depth wave spectra. In Section 5, finally, we investigate the contributions to the transfer integral from different regions of interaction phase space. These investigations are pertinent to various approximations of the exact integral expression based on the narrow-peak expansion (Longuet-Higgins, 1976; Fox, 1976; Dungey and Hui, 1979; Herterich and Hasselmann, 1980) or the local interaction expansion (Part II). The phase space analysis indicates that although these approximations capture some of the salient features of the full integral expression, they are not sufficiently accurate to serve as acceptable parameterizations in wave models, and that alternative parameterization approaches must therefore be explored.

2. Computation of the nonlinear transfer in symmetrical interaction phase space

The source function $S_{nl}(\mathbf{k})$ describing the rate of change of energy of the wave spectrum $F(\mathbf{k})$ at the wavenumber $\mathbf{k}_4$ due to nonlinear wave–wave interactions is given by the Boltzmann integral expression

$$S_{nl}(\mathbf{k}_4) = \omega_4 \int \sigma\delta(\mathbf{k}_1 + \mathbf{k}_2 - \mathbf{k}_3 - \mathbf{k}_4) \times \delta(\omega_1 + \omega_2 - \omega_3 - \omega_4)[n_1 n_2(n_3 + n_4) - n_3 n_4(n_1 + n_2)]d\mathbf{k}_1 d\mathbf{k}_2 d\mathbf{k}_3 \quad (2.1)$$

where $n_j \equiv n(\mathbf{k}_j) = F(\mathbf{k}_j)/\omega_j$ represent action densities, $\omega_j = (gk_j \tanh k_j h)^{1/2}$ $(j = 1, \cdots 4)$ wave frequencies, h is the water depth, g the gravitational acceleration, and σ represents a net scattering coefficient which is proportional to the square of a (rather complex) interaction coefficient (Hasselmann, 1962, 1963b).

Equation (2.1) describes the net energy received by a given wave component $\mathbf{k} \equiv \mathbf{k}_4$ due to interactions with all combinations of quadruplets $\mathbf{k}_1$, $\mathbf{k}_2$, $\mathbf{k}_3$, $\mathbf{k}_4$ satisfying the resonance conditions expressed by the δ-functions in the integral. The form (2.1) is not symmetrical in the four interacting wavenumber components, since the wave component $\mathbf{k}_4$ has been singled out in considering the effect of the interactions. However, the interactions as such are completely symmetrical: the scattering coefficient σ is invariant with respect to permutations of the wavenumbers, and the incremental change of action is the same (except for a simple sign rule) for all four components participating in a given interaction (principle of detailed balance, cf. Hasselmann, 1966). Thus the computation of the integrand in (2.1) for a particular infinitesimal element $d\mathbf{k}_1 d\mathbf{k}_2 d\mathbf{k}_3$ of the six-dimensional (6d) integration space yields not only the incremental rate of change of the action density at the selected wavenumber $\mathbf{k}_4$, but also the identical action changes occurring at the other three wavenumbers $\mathbf{k}_1$, $\mathbf{k}_2$ and $\mathbf{k}_3$. This additional information is disregarded in the usual method of determining S_{nl} by straightforward numerical integration of (2.1).

We adopt here an alternative technique for computing S_{nl} which exploits the basic symmetry of the interactions. The integration is carried out in the general 8d-interaction space $\mathbf{k}_1\mathbf{k}_2\mathbf{k}_3\mathbf{k}_4$, the identical incremental changes in action resulting from the interactions within an infinitesimal phase volume element $d\mathbf{k}_1 d\mathbf{k}_2 d\mathbf{k}_3 d\mathbf{k}_4$ being recorded simultaneously for all four interacting wavenumbers $\mathbf{k}_1$, $\mathbf{k}_2$, $\mathbf{k}_3$ and $\mathbf{k}_4$. The single evaluation of the general 8d-interaction integral is basically equivalent to the evaluation of the 6d-integral (2.1) for the 2d-ensemble of wavenumbers $\mathbf{k}_4$. However, the net phase volume can be reduced by a factor of 8 through the exploitation of the symmetries implied by the principle of detailed balance. A further reflection symmetry of the interaction coefficient yields an additional factor-2 saving in the calculation of the cross section σ (this is not applicable to the spectral product expression, however). Another advantage of the symmetrical integration technique is that it automatically ensures the conservation of energy, momentum and action.

The method is most easily explained and visualized in the particle picture. This provides particularly simple rules for the exchange of action, energy and momentum between resonantly interacting wave trains (cf. Hasselmann, 1966). The wave trains may be represented as finite wave packets that interact only during the finite time span in which all four wave packets occupy the same region of space. The mean exchange of action (and energy and momentum) between the wave trains during this period may be expressed in the analogous particle picture in terms of the probability of creating and annihilating "particles" or "wave packets" in a collision process. In the particle analogy, the resonant interaction between four wave components is represented as the sum of four "collision" processes between "wave packets" or particles (Fig. 1). The collision probabilities of the four processes, expressed in terms of a probability density in the 8d-wavenumber phase

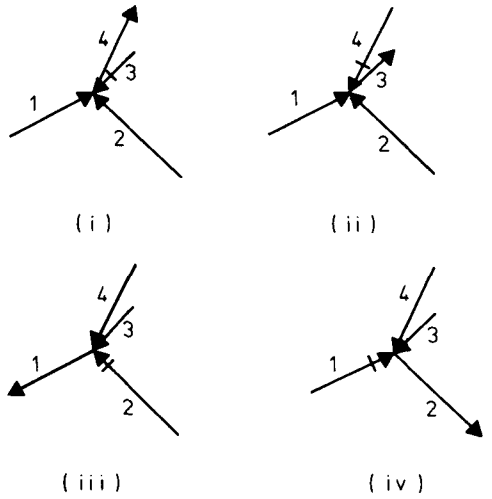

FIG. 1. The four basic collision diagrams in the particle picture for the quadruplet $\mathbf{k}_1, \mathbf{k}_2, \mathbf{k}_3, \mathbf{k}_4$ satisfying the resonance conditions $\mathbf{k}_1 + \mathbf{k}_2 = \mathbf{k}_3 + \mathbf{k}_4$, $\omega_1 + \omega_2 = \omega_3 + \omega_4$.

space of the four interacting wave components, is given by

$$\left.\begin{array}{ll}(\mathrm{i}) & n_1n_2n_3\\ (\mathrm{ii}) & n_1n_2n_4\\ (\mathrm{iii}) & n_1n_3n_4\\ (\mathrm{iv}) & n_2n_3n_4\end{array}\right\}\frac{\sigma}{4}\,\delta(\mathbf{k}_1+\mathbf{k}_2-\mathbf{k}_3-\mathbf{k}_3)$$
$$\times\,\delta(\omega_1+\omega_2-\omega_3-\omega_4)d\mathbf{k}_1d\mathbf{k}_2d\mathbf{k}_3d\mathbf{k}_4 \quad (2.2)$$

where the same scattering (collision) coefficient σ applies for all four processes. In each collision, the three ingoing particles or antiparticles are annihilated, and the outgoing particle is created. "Antiparticles" (ingoing particles associated with negative frequency and wavenumber in the resonance conditions) are denoted by cross bars in Fig. 1 and are associated with negative energy, momentum and number (action) density n. The annihilation of an antiparticle is thus equivalent to the creation of a particle. (Note that the particularly simple rules used here for writing down transfer rates for classical wave–wave interaction processes using a particle analogy differ in some important details from the normal boson particle interpretation—cf. Hasselmann, 1966). Applying these rules, the changes Δn_j in the particle number (i.e., wave action), per unit time, for each of the four wavenumbers involved in the set of four interactions of Fig. 1 are given by

$$\begin{Bmatrix}\Delta n_1\\ \Delta n_2\\ \Delta n_3\\ \Delta n_4\end{Bmatrix}=\begin{Bmatrix}-1\\ -1\\ +1\\ +1\end{Bmatrix}\cdot dW \quad (2.3)$$

where

$$dW=\tilde{\sigma}\cdot\frac{P}{4}\cdot d\mathbf{k}_1\cdot d\mathbf{k}_2\cdot d\mathbf{k}_3\cdot d\mathbf{k}_4 \quad (2.4)$$

$$\tilde{\sigma}=\sigma\delta(\mathbf{k}_1+\mathbf{k}_2-\mathbf{k}_3-\mathbf{k}_4)\delta\omega_1+\omega_2-\omega_3-\omega_4) \quad (2.5)$$

$$P=n_1n_2(n_3+n_4)-n_3n_4(n_1+n_2). \quad (2.6)$$

The integral (2.1) follows from (2.3)–(2.6) by integrating Eq. (2.3) under the side condition that one of the four wavenumbers is fixed. [A factor ¼ enters in (2.2), (2.4) because each of the four interacting wavenumbers can be chosen in turn as the fixed wavenumber.]

However, the net energy transfer rate associated with the differential form (2.4) can also be computed directly by integrating over all interactions in the full 8d-interaction space and storing the four incremental changes (2.3) of the action for each of the four wave components involved in the elementary interaction sets in the appropriate "bins" of a two-dimensional wavenumber grid. The net rate of change of the action spectral density is obtained at the end of the integration by dividing the change in action (particle number) computed for each bin by the area of the bin. A useful feature of this technique is that the wavenumber resolution of the output of the integration can be chosen independently of the integration grid.

Formally, the symmetrical integral method can be derived from (2.1) by writing $[\partial F(\mathbf{k}_4')/\partial t] = \int \delta(\mathbf{k}_4' - \mathbf{k}_4)[\partial F(\mathbf{k}_4)/\partial t]d\mathbf{k}_4$, substituting the integral expression for $\partial F(\mathbf{k}_4)/\partial t$ into the right-hand side and considering simultaneously the three similar expressions for the output wavenumbers $\mathbf{k}_1'$, $\mathbf{k}_2'$, $\mathbf{k}_3'$. Except for the "bin selection factor" $\delta(\mathbf{k}_i' - \mathbf{k}_i)$, the same integral over 8d-interaction space $d\mathbf{k}_1d\mathbf{k}_2d\mathbf{k}_3d\mathbf{k}_4$ is involved for all output wavenumbers $\mathbf{k}_1'$, $\mathbf{k}_2'$, $\mathbf{k}_3'$ and $\mathbf{k}_4'$.

In addition to the factor-8 saving derived from the symmetries, another order-of-magnitude reduction in computing time can be achieved in production runs by precomputing the cross sections and prefiltering the interaction phase space, retaining only those regions of phase space that have been established as important for a given type of spectrum in previous test computations.

The presence of the δ-functions in (2.1), (2.5) reduces the effective interaction space to a 5d-resonance hypersurface in the 8d-wavenumber space $\mathbf{k}_1\mathbf{k}_2\mathbf{k}_3\mathbf{k}_4$. Details on the removal of the δ-functions, the exploitation of symmetries, the introduction of stretched variables to provide higher resolution in important regions of the interaction space and other numerical aspects are given by Hasselmann and Hasselmann (1981).

3. Principal properties of the nonlinear transfer

Since numerical computations of the nonlinear transfer S_{nl} for various types of deep water spectra have been published by a number of workers (Hasselmann, 1963b; Snodgrass *et al.*, 1966; Sell and Hasselmann, 1972; Hasselmann *et al.*, 1973; Webb, 1978; Masuda, 1981) we limit ourselves here to a summary of the principal properties of the source function S_{nl}, referring

to Hasselmann and Hasselmann (1981) and Young *et al.* (1985b) for more extensive compilations of computations. A satisfactory simulation of these features is an important requirement for the parameterization schemes discussed in Part II. We consider the modifications induced by finite depth in Section 4.

1) For a two-dimensional spectrum

$$F(f, \varphi) = \frac{\alpha g^2}{(2\pi)^4} f_m^{-5} \hat{F}(\nu, \varphi)$$

(f = frequency, φ = wave propagation direction) (3.1)

characterized by the frequency and energy scale parameters f_m and α, respectively, and with a given spectral shape $\hat{F}(\nu, \varphi)$, where $\nu = f/f_m$, the nonlinear transfer scales as

$$S_{nl}(f, \varphi) = \alpha^3 g^2 f_m^{-4} \hat{S}_{nl}(\nu, \varphi) \quad (3.2)$$

where $\hat{S}_{nl}$ is a nondimensional distribution that is determined by the corresponding nondimensional distribution $\hat{F}$ and is independent of the scale parameters (for finite depth waves, $\hat{S}_{nl}$ depends also on the nondimensional depth parameter hf_m^2/g). f_m is usually taken as the frequency of the peak of the spectrum and α (where applicable) as Phillips' constant. An alternative scaling which is sometimes useful is

$$S_{nl}(f, \varphi) = g^{-4} \epsilon^3 f_m^{\ 8} \hat{S}_{nl}(\nu, \varphi) \quad (3.3)$$

where $\epsilon = \int\int F(f, \varphi) df d\varphi$ represents the total wave energy (mean square surface displacement).

2) S_{nl} typically has a 3-lobed positive–negative–positive distribution. For a fully developed Pierson-Moskowitz spectrum, the low-frequency positive lobe is located roughly at the spectral peak, while for a growing wind-sea spectrum of the more sharply peaked JONSWAP form the low-frequency positive lobe lies slightly to the left of the peak on the forward face of the spectrum (cf. II, Fig. 1). The nonlinear transfer is approximately an order of magnitude larger for the JONSWAP spectral shape than for the Pierson-Moskowitz form. The strong dependence of the position and magnitude of the positive lobe on the shape of the spectrum is an important feature governing the evolution of the wind wave spectrum.

3) The high-frequency positive lobe tends to have a broader directional distribution than the other two lobes. This is presumably one of the reasons for the observed broadening of the spectral spreading function towards higher frequencies.

4) The low frequency positive lobe is concentrated in a narrow frequency band and also has a relatively narrow directional distribution. There is a tendency to develop relative maxima within this lobe on either side of the mean propagation direction. This feature has been discussed for the narrow-peak approximation by Longuet-Higgins (1976) and Fox (1976) and is responsible for the horseshoe-shaped isoline structure of the theoretical fully developed two-dimensional spectrum obtained by numerical integration of the spectral energy balance equation (cf. Komen *et al.*, 1984).

5) The interactions are relatively short range in wavenumber space (cf. also Section 5, and Part II, Section 4). Thus the strongest transfer rates are found rather close to the spectral peak, particularly for sharply peaked spectra. The interaction between a wind sea and swell is normally negligible, unless the swell frequency is so high that it falls within the wind-sea frequency range (i.e., the swell has comparable wavelength to the wind sea but is propagating in a different direction). In this case the swell is rapidly absorbed in the wind sea (cf. Young *et al.*, 1985b).

4. Finite depth effects

Equation (2.1) holds generally for a wave spectrum in any water depth, provided the interactions can still be regarded as weak, i.e., provided the interaction time $\tau_{\text{int}} = F/S_{nl}$ is large compared with a characteristic spectral time scale τ_{sp} defined by the inverse of the peak width of the frequency spectrum. (The relevant spectral time scale τ_{sp} is governed by the width of the spectrum rather than a characteristic mean frequency, since the usual weak-interaction two-time scale approximation involves replacing a narrow finite-time resonance response function by a frequency δ-function.) Since, with the exception of the report by Hasselmann and Hasselmann (1981), previously published computations of the nonlinear transfer have been limited to the infinite depth case, we discuss here a few results for finite depth spectra. [We note that in the original expression for the finite-depth interaction cross section given by Hasselmann (1962), two terms were overlooked; the correct expression is given by Herterich and Hasselmann (1980, Appendix B)].

To compare the finite depth case with the infinite depth results, the source functions S_{nl} were computed for a series of identical spectra $F(f, \theta)$ for different water depths. As reference spectrum we chose a JONSWAP spectrum with a Mitsuyasu-Hasselmann-type frequency-dependent spreading function [cf. II, Eqs. (2.1)–(2.5), and Fig. 4a].

Figures 2a–f show the one-dimensional distribution $S_{nl}(f)$ for various values of the depth parameter $k_m h$, where k_m is the wavenumber corresponding to the peak frequency $f_m = \omega_m/2\pi$ as given by the dispersion relation $\omega_m^{\ 2} = g k_m \tanh k_m h$. Also shown in each panel is the corresponding deep-water source function S_{nl}^{∞}, rescaled by a factor R' such that $R' S_{nl}^{\infty} = \hat{S}_{nl}^{\infty}$ agrees as closely as possible with the finite-depth source function. For $k_m h \geq 0.8$ the shape of the finite-depth source function S_{nl} is seen to be very similar to the shape of the infinite-depth source function, although at $k_m h$

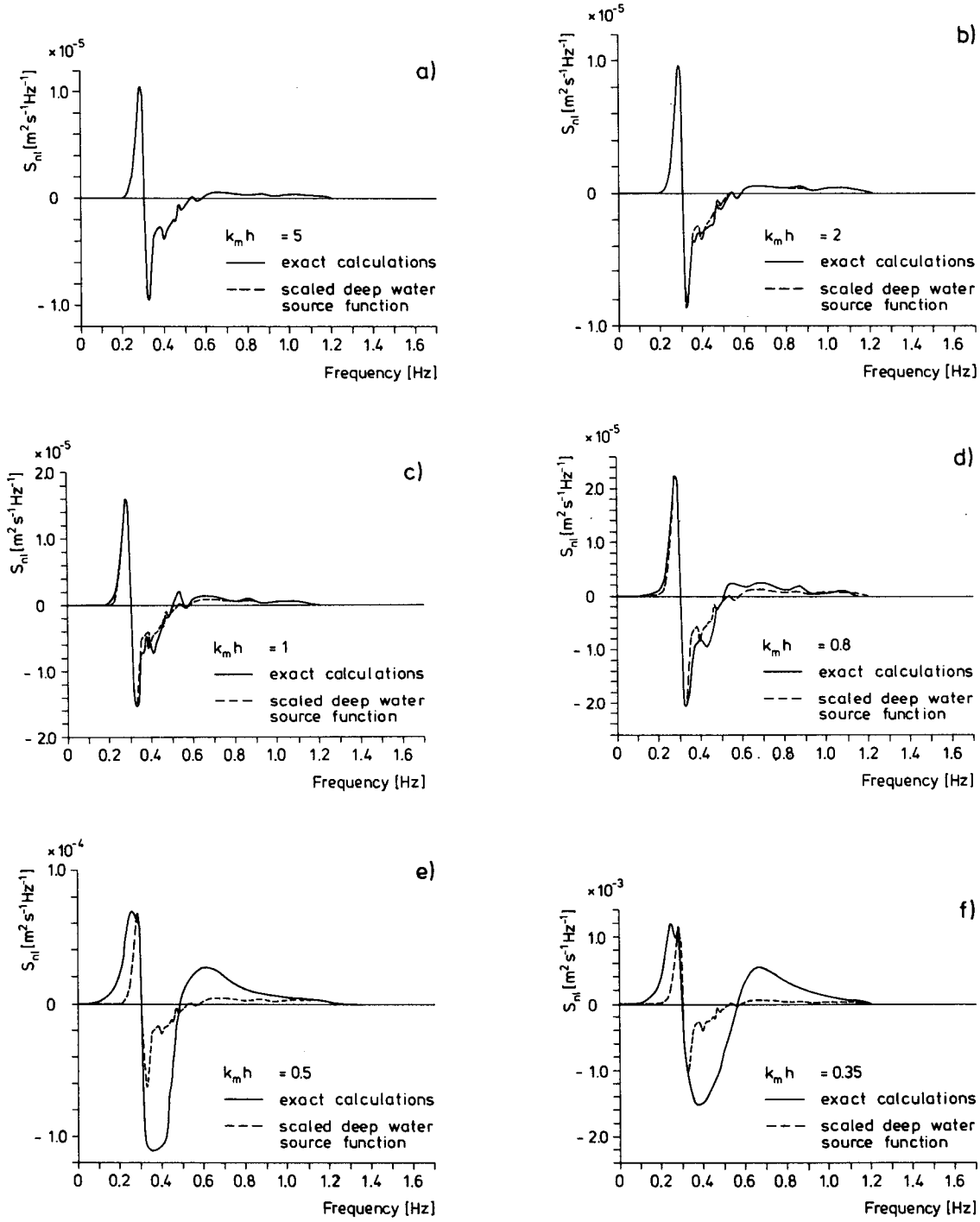

FIG. 2. One-dimensional source functions S_{nl} computed for different water depths for a JONSWAP spectrum with a Mitsuyasu-Hasselmann spreading factor (cf. Fig. 4a). Also shown are the appropriately scaled source functions S_{nl}^{∞} for infinite depth.

= 0.8 the magnitude is already twice that of the infinite depth case. The shape similarity holds also for the directional distributions (not shown here, cf. Hasselmann and Hasselmann, 1981). These results are consistent with the conclusions of Herterich and Hasselmann (1980) based on similarity arguments for the narrow-peak approximation. However, the increase of the factor R' with decreasing $k_m h$ is greater for the exact computations than inferred from the narrow-peak approximation (cf. Fig. 3).

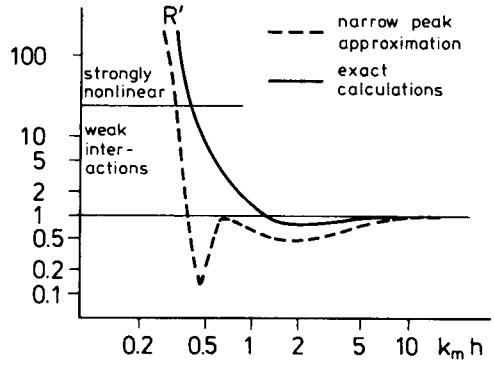

FIG. 3. Ratios R' of the nonlinear transfer for finite-depth and infinite-depth wave spectra as inferred from the exact computations of Fig. 2 and as derived from the narrow-peak approximation (from Herterich and Hasselmann, 1980).

For $k_m h \leqslant 0.4$ the nonlinear transfer exceeds the deep water values by more than an order of magnitude, and the weak nonlinear approximation becomes questionable (Fig. 3). This is also the region in which the distortions in the distribution of S_{nl} become most pronounced. However, the general three-lobe structure of the transfer function is retained for all $k_m h$ values (as required by the simultaneous conservation of energy and action), and it may therefore be concluded that the effect of the nonlinear transfer on the evolution of the wave spectrum is qualitatively similar in the finite depth and infinite depth cases.

Instead of relating the finite depth calculations to the infinite depth case through a fixed reference frequency spectrum we could also have chosen a fixed reference spectrum with respect to wavenumber. This would be more in keeping, for example, with various scaling hypotheses for the high-wavenumber region of the spectrum (Phillips, 1958; Kitaigorodskii *et al.*, 1975; Kitaigorodskii, 1983; Bouws *et al.*, 1985a,b). However, a wavenumber reference spectrum is perhaps less appropriate for the energy containing region of the spectrum, since it shifts the finite-depth peak frequency to lower values than the deep water value, whereas the opposite is observed empirically. The choice of reference spectrum is essentially arbitrary, since the structure of the energy balance in terms of the input, dissipation and nonlinear transfer processes cannot in general be expected to be simply related for the infinite depth and finite depth cases (cf. Bouws and Komen, 1983).

For a wavenumber reference spectrum, the theoretical scaling factor R' for the narrow-peak approximation is found to be reduced by a factor $(\tanh k_m h)^{9/2}$. (The same scaling factors may be expected to apply to first order also for the local-interaction approximation discussed in II). If this factor is applied to the R' curve of Fig. 3, the finite-depth nonlinear transfer is found to be significantly depressed below the infinite depth value in the region $0.5 < k_m h < 1.5$. If the nonlinear transfer plays a similarly significant role in the energy balance of finite-depth waves as in the infinite depth case, a universal, depth-independent scaling of the wavenumber spectrum cannot hold. We should expect qualitatively a depth scaling intermediate between a depth-independent frequency and a depth-independent wavenumber spectrum.

5. Contributions to the Boltzmann integral from different regions of interaction phase space

Various approximations of the full Boltzmann interaction integral have been proposed on the premise that only limited subregions of the full interaction space contribute significantly to the integral. In the local interaction approximation (Part II) the dominant interaction region is assumed to lie in the vicinity of the center point $\hat{\mathbf{k}} = (\mathbf{k}_1 + \mathbf{k}_2)/2 = (\mathbf{k}_3 + \mathbf{k}_4)/2$ of Longuet-Higgins's "figure-of-eight" interaction diagram (cf. Hasselmann, 1963b; and II, Fig. 6), while in the narrow-peak approximation (Longuet-Higgins, 1976; Fox, 1976; Dungey and Hui, 1979; Herterich and Hasselmann, 1980) only interactions in the neighborhood of the spectral peak $\mathbf{k}_m$ are considered. The latter restriction automatically ensures that all interacting wavenumbers also lie in the neighborhood of $\hat{\mathbf{k}}$, and that $\hat{\mathbf{k}} \approx \mathbf{k}_m$. In the local-interaction approximation, on the other hand, $\hat{\mathbf{k}}$ is free to vary throughout the 2d-wavenumber plane. The two approximations also differ in the assumptions and details of the expansions (sharply peaked cross sections in the first case, sharply peaked spectra in the second). In this section we investigate the basic assumptions of the two approximations regarding the importance of particular regions of interaction space, without entering into the details of the expansion procedures. As reference spectrum we choose the same JONSWAP spectrum with a Mitsuyasu-Hasselmann spreading function as in the previous section.

Figure 4 shows the two-dimensional wave spectrum (panel a), the complete integral computation of S_{nl} (panel b) and two filtered integral computations appropriate for the local interaction approximation, in which only those wavenumber quadruplets are retained for which all components lie within circles $|\mathbf{k}_i - \hat{\mathbf{k}}| < |\hat{\mathbf{k}}|/2$ (panel c) or $|\mathbf{k}_i - \hat{\mathbf{k}}| < |\hat{\mathbf{k}}|/4$ (panel d) around $\hat{\mathbf{k}}$. While panel c still indicates a reasonably good agreement with the exact calculation of panel b, panel d shows that if the interaction region is restricted further to a 25% radius circle around $\hat{\mathbf{k}}$, the nonlinear transfer is strongly reduced to about $1/5$ of its exact value. Since a limitation to a radius of this order of magnitude is needed to apply the higher-order differential diffusion operator resulting from the local-interaction expansion with some confidence, it is not surprising that this approximation exhibits deficiencies. Even if the local-interaction result is rescaled to agree in magnitude with the exact computations, the shape of the 3-lobe distri-

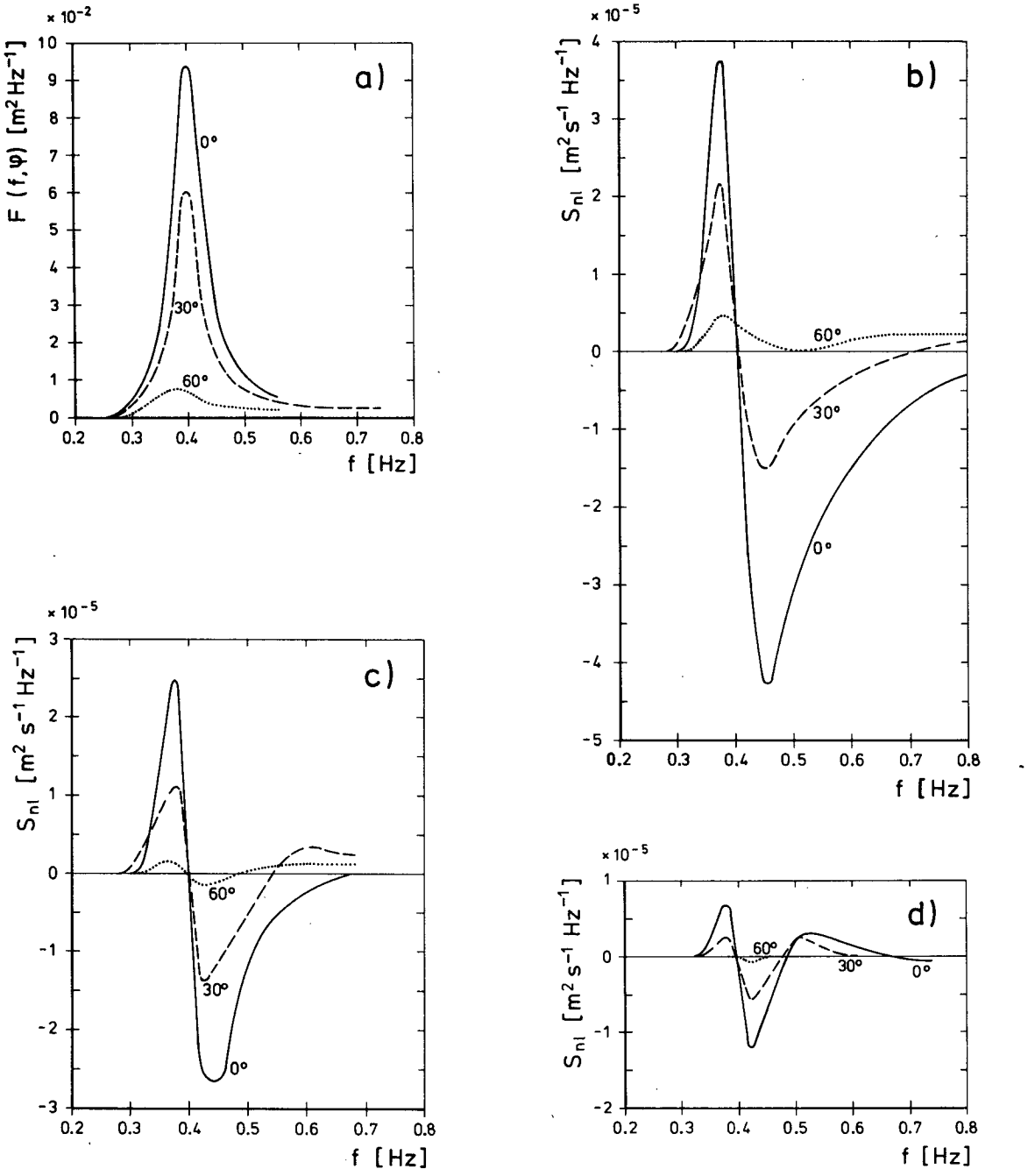

FIG. 4. Two-dimensional wave spectrum (panel a) and source functions computed by integrating over the full interaction space (panel b) and over limited regions $|\mathbf{k}_i - \hat{\mathbf{k}}| < |\hat{\mathbf{k}}|/2$ (panel c) and $|\mathbf{k} - \hat{\mathbf{k}}| < |\hat{k}|/4$ (panel d) around the central interaction wavenumber $\hat{\mathbf{k}}$.

bution in panel d is seen to be too narrow. This is, indeed, precisely one of the shortcomings evident in the diffusion-operator parameterization (cf. Part II). Panel d also explains another deficiency of the diffusion-operator approximation: the ratios of the values of S_{nl} obtained for strongly peaked (fetch limited JONSWAP) spectra relative to less strongly peaked (fully developed Pierson-Moskowitz) spectra are too large. This comes about because for sharply peaked spectra a larger proportion of the transfer is provided by the interactions in the neighborhood of the peak, which are retained in the local-interaction approximation.

A comparison of panels c and d, finally, explains why the alternative discrete-interaction parameterization (cf. Part II) is more successful. The dominant contribution to the nonlinear transfer is clearly provided

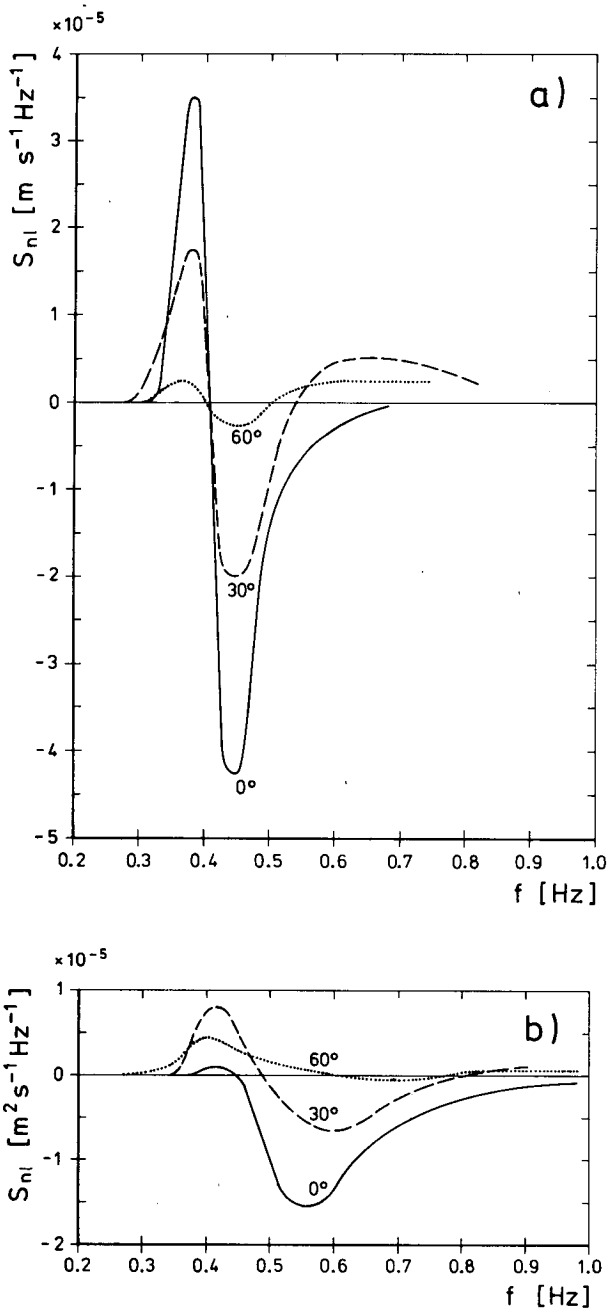

FIG. 5. Complementary contributions to the complete source function shown in Fig. 4b from interactions involving at least one wavenumber $\mathbf{k}_i$ in the vicinity of the spectral peak $\mathbf{k}_m$, $|\mathbf{k}_i - \mathbf{k}_m| < |\mathbf{k}_m|/4$ (panel a) and interactions involving no wavenumber in the vicinity of the peak, $|\mathbf{k}_i - \mathbf{k}_m| > |\mathbf{k}_m|/4$ for all $\mathbf{k}_i$ (panel b).

by the interactions in the $k_m/2$-circle region of panel c, but excluding the $k_m/4$-region of panel d, i.e., by interactions in the "ring" region

$$\left.\begin{aligned} |\mathbf{k}_i - \hat{\mathbf{k}}_m| &> \hat{k}_m/4 \quad \text{for at least one } \mathbf{k}_i \\ |\mathbf{k}_i - \hat{\mathbf{k}}_m| &< k_m/2 \quad \text{for all } \mathbf{k}_i \end{aligned}\right\}.$$

The optimal interaction configurations derived (empirically) for the discrete-interaction parameterization are found to lie precisely in this ring region.

The contributions from the different phase-space regions relevant for the narrow-peak approximation are shown in Fig. 5. Panel a shows the nonlinear transfer resulting from all interactions involving the spectral-peak region (at least one $\mathbf{k}_i$ in the region $|\mathbf{k}_i - \mathbf{k}_m| < |k_m|/4$) while panel b shows the contribution from the complementary set of interactions in which none of the wavenumbers lies in the peak region ($|\mathbf{k}_i - \mathbf{k}_m| > |k_m|/4$ for all $\mathbf{k}_i$). The sum of these two contributions yields the total transfer shown in Fig. 4b.

As expected, the interactions involving the peak reproduce the exact expression very well in the neighborhood of the peak, while the complementary set of interactions captures most of the transfer at high wavenumbers, where the net transfer is quasi-local in wavenumber space (cf. Hasselmann, 1963b). However, in the important transition region $1.2\omega_m \leqslant \omega \leqslant 1.5\omega_m$, which normally contains a large fraction of the total wind input and dissipation (cf. Komen *et al.*, 1984), the contributions from both types of interaction are comparable. Although this analysis does not mirror the narrow-peak approximations exactly (these require more strictly that not just one, but all interacting wavenumbers lie in the neighborhood of the peak, while on the other hand the peak can extend beyond the sharp limits defined here) it appears that the narrow-peak approach is too restricted for a general simulation of the full spectral energy balance, including both processes in the peak region and the coupling between the peak region and the higher-wavenumber range in which most of the dissipation takes place.

Acknowledgments. This work was partly supported by the Office of Naval Research under Contract N00014-77-9-0054 and the European Space Agency under Contract 5544/83/F/CG.

REFERENCES

Bouws, E., and G. J. Komen, 1983: On the balance between growth and dissipation in an extreme depth-limited wind sea in the southern North Sea. *J. Phys. Oceanogr.*, **13**, 1653–1658.

——, H. Günther, W. Rosenthal and C. L. Vincent, 1985a: Similarity of the wind wave spectrum in finite depth water. Part I: Spectral form. *J. Geophys. Res.*, **90**, 975–986.

——, ——, —— and ——, 1985b: Similarity of the wind wave spectrum in finite depth water. Part II: Statistical relations between shape and growth stage parameters. *J. Geophys. Res.*, (submitted).

Cartwright, D. E., 1968: Computations of the nonlinear energy transfer for a Pierson-Moskowitz spectrum. (unpublished report).

Dungey, J. C., and W. H. Hui, 1979: Nonlinear energy transfer in a narrow gravity-wave spectrum. *Proc. Roy. Soc. London*, **A368**, 239–265.

Fox, M. J. H., 1976: On the nonlinear transfer of energy in the peak of a gravity-wave spectrum II. *Proc. Roy. Soc. London*, **A348**, 467–483.

Hasselmann, K., 1962: On the nonlinear energy transfer in a gravity-wave spectrum. Part 1: General theory. *J. Fluid Mech.*, **12**, 481–500.

——, 1963a: On the nonlinear energy transfer in a gravity-wave spectrum. Part 2: Conservation theorems, wave-particle correspondence, irreversibility. *J. Fluid Mech.*, **15,** 273–281.

——, 1963b: On the nonlinear energy transfer in a gravity-wave spectrum. Part 3: Computation of the energy flux and swell-sea interaction for a Neumann spectrum. *J. Fluid Mech.*, **15,** 385–398.

——, 1966: Feynman diagrams and interaction rules of wave–wave scattering processes. *Rev. Geophys.*, **4,** 1–32.

——, and Collaborators, 1973: Measurements of wind-wave growth and swell decay during the Joint North Sea Wave Project (JONSWAP). *Dtsch. Hydrogr. Z.* **A8,** 95 pp.

Hasselmann, S., and K. Hasselmann, 1981: A symmetrical method of computing the nonlinear transfer in a gravity-wave spectrum. *Hamb. Geophys. Einzelschriften, Reihe A: Wiss. Abhand.*, **52,** 138 pp.

——, and ——, 1985: The wave model Exact-NL. *Ocean Wave Modeling,* (The SWAMP Group), Plenum, 256 pp.

——, ——, J. H. Allender and T. P. Barnett, 1985: Computations and parameterizations of the nonlinear energy transfer in a gravity wave spectrum. Part II: Parameterizations of the nonlinear energy transfer for application in wave models. *J. Phys. Oceanogr.*, **15,** 1378–1391.

Herterich, K., and K. Hasselmann, 1980: A similarity relation for the nonlinear energy transfer in a finite-depth gravity-wave spectrum. *J. Fluid Mech.*, **97,** 215–224.

Kitaigorodskii, S. A., 1983: On the theory of the equilibrium range in the spectrum of wind-generated gravity waves. *J. Phys. Oceanogr.*, **13,** 816–827.

——, V. P. Krasitskii and M. M. Zaslayskii, 1975: On Phillips' theory of equilibrium range in the spectra of wind-generated gravity waves. *J. Phys. Oceanogr.*, **5,** 410–420.

Komen, G. J., S. Hasselmann and K. Hasselmann, 1984: On the existence of a fully developed wind-sea spectrum. *J. Phys. Oceanogr.*, **14,** 1271–1285.

Longuet-Higgins, M. S., 1976: On the nonlinear transfer of energy in the peak of a gravity-wave spectrum. *Proc. Roy. Soc. London,* **A347,** 311–328.

Masuda, A., 1981: Nonlinear energy transfer between wind waves. *J. Phys. Oceanogr.*, **10,** 2082–2093.

Phillips, O. M., 1958: The equilibrium range in the spectrum of wind-generated ocean wave. *J. Fluid Mech.*, **4,** 426–434.

Sell, W., and K. Hasselmann, 1972: Computations of nonlinear energy transfer for JONSWAP and empirical wind-wave spectra. Rep. of the Institute of Geophysics, University of Hamburg, 125 pp.

Snodgrass, F. E., G. W. Groves, K. F. Hasselmann, G. R. Miller, W. H. Munk and W. H. Powers, 1966: Propagation of ocean swell across the Pacific. *Phil. Trans. Roy. Soc. London,* **A259,** 431–497.

The SWAMP Group, 1985: Sea Wave Modelling Project (SWAMP). An intercomparison study of wind wave prediction models, Part 1: Principal results and conclusions. *Ocean Wave Modeling,* Plenum, 256 pp.

Webb, D. J., 1978: Nonlinear transfer between sea waves. *Deep-Sea Res.*, **25,** 279–298.

Young, I. R., S. Hasselmann and K. Hasselmann, 1985a: Computations of the response of a wave spectrum to a sudden change in the wind direction, (in preparation).

——, —— and ——, 1985b: Calculations of the nonlinear interactions in cross seas. *Hamb. Geophys. Einzelschriften,* **74,** 49 pp.